Strongly photoreducing organic donor-acceptor thermally activated delayed fluorescence photocatalysts

Megan Amy Bryden,[a] Ettore Crovini,[a] Thomas Comerford,[a] Armido Studer*,[b] and Eli Zysman-Colman*,[a]

[a] Organic Semiconductor Centre, EaStCHEM School of Chemistry, University of St Andrews, St Andrews, Fife, U.K., KY16 9ST, Fax: +44-1334 463808; Tel: +44-1334 463826;
E-mail: eli.zysman-colman@st-andrews.ac.uk;
URL: http://www.zysman-colman.com
[b] University of Münster, Organisch-Chemisches Institut, Corrensstaße 40, 48149 Münster.

Abstract

We report a family of donor-acceptor thermally activated delayed fluorescent (TADF) compounds based on derivatives of **DMAC-TRZ**, that are strongly photoreducing. Both E_{ox} and thus E^*_{ox} could be tuned via substitution of the DMAC donor with a Hammett series of *p*-substituted phenyl moieties while E_{red} remained effectively constant. These compounds were assessed in the photoinduced dehalogenation of aryl halides, and analogues bearing electron withdrawing groups were found to produce the highest yields. Substrates of up to E_{red} = -2.72 V could be dehalogenated at low PC loading (1 mol%) and under air, conditions much milder than previously reported for this reaction. Spectroscopic and chemical studies demonstrate that all PCs, including literature reference PCs, photodegrade, and that it is these photodegradation products that are responsible for the reactivity.

Introduction

Photocatalysis has evolved over the last 15 years to be a popular and effective methodology of organic synthesis, enabling the formation of compounds that would otherwise be inaccessible using traditional thermal synthesis.[1–3] Moreover, photocatalysis is arguably a "greener" route of synthesis compared to other methods as conditions are generally less harsh (ambient temperature and pressure) and often avoids the use of toxic stoichiometric oxidants and/or reductants, in favour of catalytic amounts of the electron transfer agent, the photocatalyst (PC).

Particularly, the mild generation of aryl radicals using photocatalysis has received significant interest,[4] especially since classic methods of forming these species from aryl halides involve stoichiometric reagents such as AIBN/*n*-Bu_3SnH.[5,6] Instead, in photocatalysis, low loadings of the PC is used to directly photoreduce the aryl halide, releasing a reactive aryl radical. However, reduction of aryl halides can be challenging and requires a strong photoreductant for scission of the C-X bond. A small series of organic PCs have been reported to initiate photoinduced dehalogenation of aryl halides over the last 10 years,[7–15] a selection of which are shown in Figure **1a**. Both *N,N*-bis(2,6-di*iso*propylphenyl)perylene-3,4,9,10-bis(dicarboximide) (**PDI**)[7] and 10-phenylphenothiazine (**PTH**)[8] (Figure **1a**) could dehalogenate aryl iodides with both electron-withdrawing groups (EWGs) $E_{red} \approx$ -1.0 – -1.7 V vs SCE[10,16,17] and electron-donating groups (EDGs) $E_{red} >$ -2.3 V vs SCE,[18] but could only dehalogenate aryl bromides and chlorides with EWGs present $E_{red} \approx$ -1.80 – -2.0 V vs SCE;[19] exceptionally, **PTH** could dehalogenate 2-bromophenol in a low yield (23% over 72 h). Both **PDI** and **PTH** were used at 5 mol% loading, typically under a N_2 atmosphere (Figure **1b**), although **PTH** was shown to be somewhat tolerant to air (94 to 68% yield under N_2 and air, respectively, in the dehalogenation 4-chlorobenzonitrile).

Recently, significant progress in the dehalogenation of aryl bromides and chlorides containing EDGs ($E_{red} <$ -2.50 V vs SCE)[20] has been achieved. Notably, Nicewicz and co-workers used an acridinium salt 3,6-di-*tert*-butyl-9-mesityl-10-phenylacridin-10-ium tetrafluoroborate, hereby named **[^{t}Bu-Mes-Acr]BF_4** (Figure **1c**)[9] to achieve yields of 58-99% over a wide scope of aryl bromides and chlorides containing EDGs; however, a high 10 mol% PC loading was required (Figure **1b**). Cyanoarene based PCs, including 1,2,3,5-tetrakis(carbazol-9-yl)-4,6-dicyanobenzene, **4CzIPN**, and related derivatives (Figure **1a**),[10,11] have been used in dehalogenation reactions, involving aryl bromides and chlorides with EDGs in yields ranging from 38-74% for direct dehalogenation[10] and 20-90% in coupling reactions.[11] Significant photon flux in the form of two or four LEDs (2 × 40 W[11] or 4 × 3 W[10]), and a PC loading of 5 mol% were used to attain these yields (Figure **1b**).[21]

a)

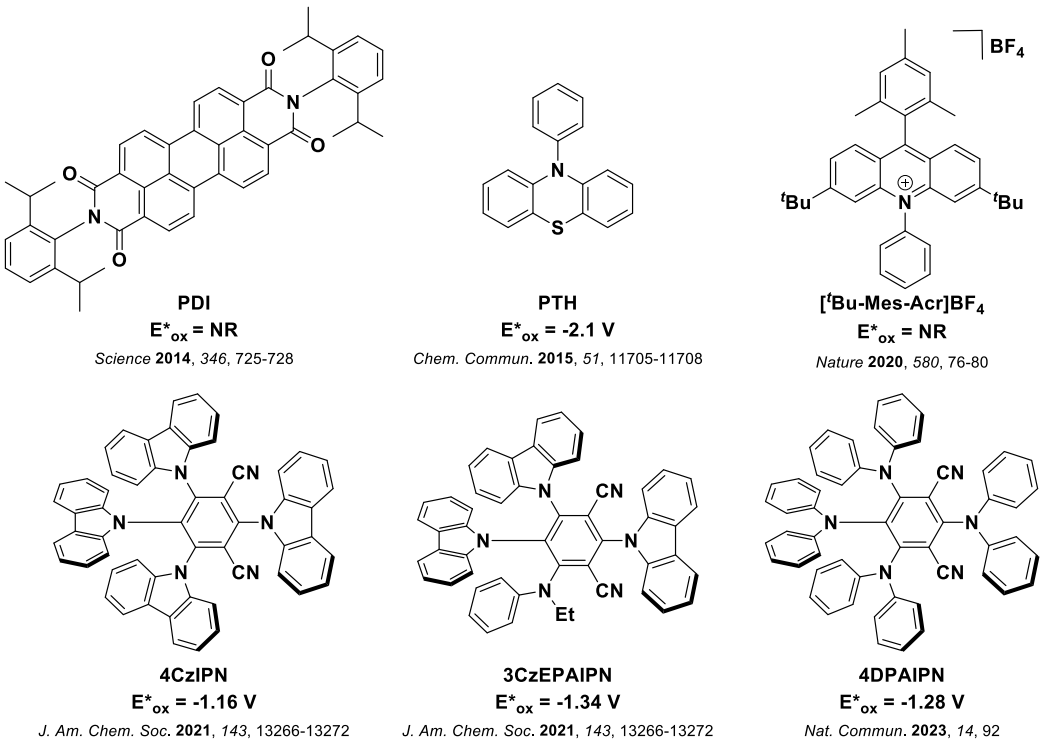

b)

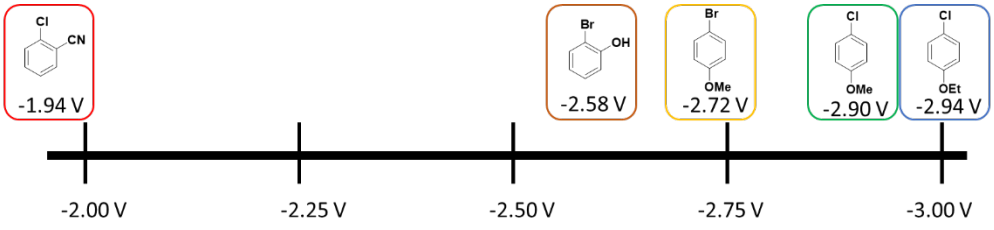

	Ref 7	Ref 8	This work	Ref 9 (Ref 10)	Ref 11
PC (mol%)	PDI (5)	PTH (5)	CNPh-DMAC-TRZ (1)	[^{t}Bu-Mes-Acr]BF_4 (10) (4DPAIPN (3))	3CzEPAIPN (5)
Solvent	DMF	MeCN	DMF	MeCN (MeCN)	MeCN
Wavelength / nm	455	380	390	390 (455 x 4)	456 x 2
Amine	NEt_3	NBu_3 (+ HCO_2H)	DIPEA	DIPEA (DIPEA)	DIPEA (+ other additives in coupling reactions)
Aeration	N_2	N_2	Air	N_2 (Argon)	Argon
Time / h	8	72	72	16 (48)	24

Figure **1**. a) A selection of organic PCs used in the literature for photoinduced dehalogenation of aryl halides and b) a summary of the most difficult substrates that can be reduced using these PCs and for the PC used in this work, as well as the conditions for that specific substrate. References given are related to the relevant dehalogenation literature. NR = not reported. Redox potentials quoted vs SCE and taken from Ref [16,18–20,22,23].

The proposed mechanisms for such photoinduced dehalogenation involve either an oxidative quenching cycle or a consecutive photoinduced electron transfer (conPET) process.

In the former, direct photoreduction of the aryl halide occurs from the PC*, with closure of the photocatalytic cycle proceeding through oxidation of the sacrificial amine by $PC^{\bullet+}$. In contrast, the conPET mechanism involves reductive quenching of the PC* by the sacrificial amine, generating $PC^{\bullet-}$, which itself is then photoexcited. The $[PC^{\bullet-}]$* then reduces the aryl halide, regenerating the ground state PC.

Of the organic PCs discussed, only **PTH** has been proposed to dehalogenate aryl halides through an oxidative quenching cycle, this based on Stern-Volmer quenching studies that showed only iodobenzene could quench the emission of **PTH**, while no discernible quenching was observed with NBu_3.[8] However, the excited state oxidation potential, E^*_{ox}, of **PTH** is quoted as -2.10 V vs SCE, yet **PTH** was shown to dehalogenate 2-bromophenyl (E_{red} = -2.58 V vs SCE),[20] a transformation which would be considerably endergonic. **PDI**, **[^{t}Bu-Mes-Acr]BF_4** and **3CzEPAIPN** (and related derivatives) have all been suggested to operate via the conPET mechanism. The evidence to support this stems from the quadratic dependency of yield with light irradiation intensity, and the direct detection of $PC^{\bullet-}$, by EPR spectroscopy, as an intermediate in the photocatlysis.[11]

Despite the advances that have been made in the photoinduced dehalogenation of aryl halides, the reaction conditions employed often use high organic PC loading (5-10 mol%) and multiple light sources. As part of a larger research effort devoted to the design of highly photooxidizing and photoreducing PCs, we sought to demonstrate the utility of a new family of donor-acceptor TADF compounds as PCs that would be capable of promoting the photoinduced dehalogenation of aryl halides under milder reaction conditions.

TADF compounds have received steadily increasing interest for their use as PCs,[24–27] particularly **4CzIPN** which has been documented as a PC in >600 literature reports.[28] TADF compounds are typically composed of donor and acceptor units that are electronically weakly coupled, usually due to a strongly twisted conformation.[29] Thus, modifications of the donor and acceptor motifs adjust the HOMO and LUMO levels, respectively, facilitating a facile tuning of the optoelectronic properties of the compounds. With this in mind, we focused on 10-(4-(4,6-diphenyl-1,3,5-triazin-2-yl)phenyl)-9,9-dimethyl-9,10-dihydroacridine, **DMAC-TRZ** (Figure **2a**). First developed in 2015 as a sky-blue emitter for organic light-emitting devices,[30] **DMAC-TRZ** is composed of a DMAC donor connected to a triazine acceptor. We identified **DMAC-TRZ** as a potentially useful photoreductant as it has a moderate optical gap ($E_{0,0}$ = 2.50 eV in DMF), and ground-state oxidation potential (E_{ox} = 0.97 V vs SCE in DMF), leading

to an E^*_{ox} of -1.53 V (*c.f.* E^*_{ox} = -1.7 V vs SCE for *fac*-Ir(ppy)$_3$),[8] which is more photoreducing than all but one of the organic PCs shown in Figure **1**. Additionally, it is commercially available at a significantly lower price than **4CzIPN (**£147.00 for 200 mg compared to £864.00 per 250 mg for **4CzIPN**).[31] Due to the near orthogonal conformation adopted by the donor, the oscillator strength for the lowest energy charge-transfer (CT) transition is exceedingly low, which translates into a low-intensity low-energy absorption band (λ_{abs} = 381 nm, ε = 2000 M^{-1} cm^{-1} in DMF).

To rationally and progressively tune the optoelectronic properties of this compound, we developed a family of analogues where the DMAC donor was substituted at the 2- and 7-positions with a Hammett series of 4-substituted phenyl moieties (Figure **2b**).[32] This substitution of the donor group should affect E_{ox}, $E_{0,0}$, and thus E^*_{ox}.

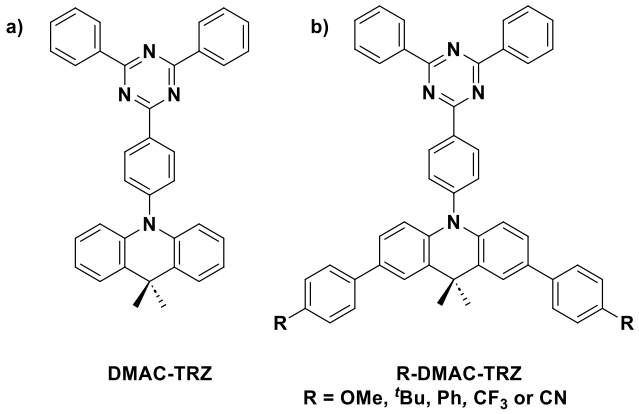

Figure **2**. Structures of a) **DMAC-TRZ** and b) functionalized **DMAC-TRZ** derivatives.

Results and Discussion

We first ascertained the optoelectronic properties of the **DMAC-TRZ** derivatives in *N,N*-dimethylformamide (DMF), a solvent that is frequently used in dehalogenation reactions in the literature; the poor solubility of these **DMAC-TRZ** derivatives in acetonitrile precluded its use. The UV-Vis absorption spectrum of **DMAC-TRZ** (Figure **3a**) matches that previously recorded in toluene,[30] displaying a weak band between 350 – 450 nm, assigned to the intramolecular CT transition from DMAC to TRZ. Excluding **CNPh-DMAC-TRZ**, the other four derivatives display a weak low-energy CT absorption band that maintains a similarly low ε to **DMAC-TRZ** (Figure **3a**); however, when changing the DMAC substituent from EWG to EDG, the onset of the CT band progressively red-shifts. All five derivatives have a more red-shifted onset relative to **DMAC-TRZ** indicating that there is increased conjugation within the donor.

In addition to this CT band, the absorption spectra of the five **DMAC-TRZ** derivatives have a well-defined band between 335 – 378 nm, which is assigned to a locally-excited (^{1}LE) transition on the substituted DMAC donor.[33] Unlike the trend for the CT band, the LE band becomes more red-shifted when moving from EDG to EWG on the DMAC donor (*e.g.*, λ_{abs} = 335 and 378 nm for **OMePh-DMAC-TRZ** and **CNPh-DMAC-TRZ**, respectively). The LE band is approximately ten-fold more intense than the CT peak (36×10^3 and 2.1×10^3 M^{-1} cm^{-1} for the LE and CT peaks, respectively, for **^{t}BuPh DMAC-TRZ**) allowing for the substituted **DMAC-TRZ** derivatives to be more absorptive at 390 nm than the parent **DMAC-TRZ**.

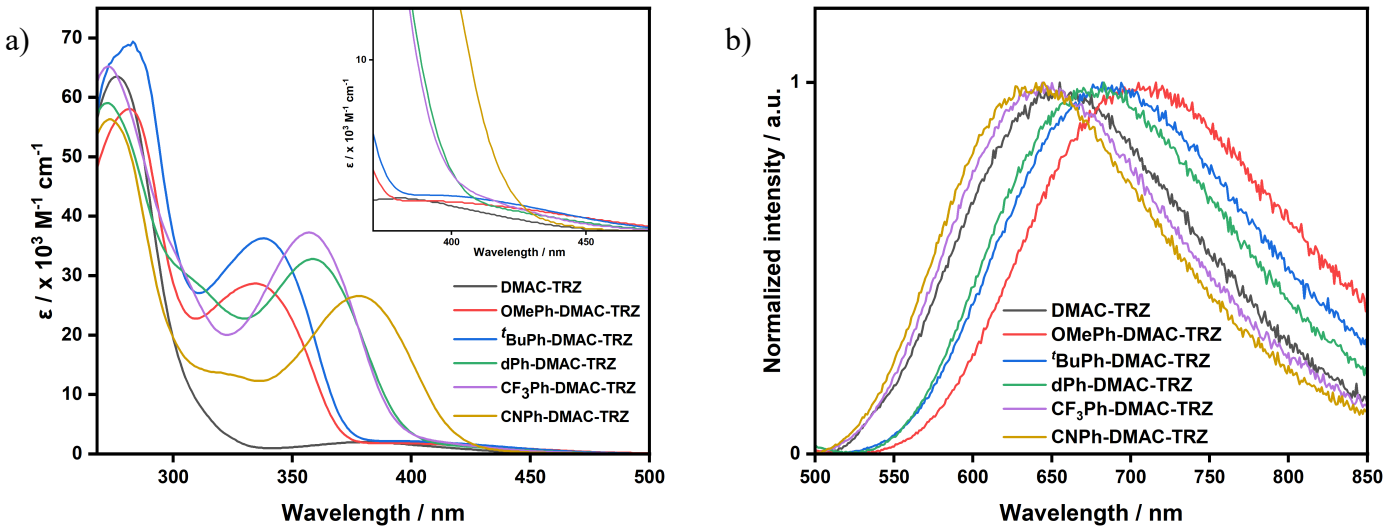

Figure **3**. a) UV-vis absorption and b) steady-state PL of **DMAC-TRZ** and derivatives obtained in DMF under air.

Steady-state photoluminescence (PL) spectra in DMF for the five **DMAC-TRZ** derivatives (Figure **3b** and Table **1**) are broad and Gaussian-shaped, indicative of emission from a CT state. The emission progressively red-shifts across the family in a similar manner to the CT band in the absorption spectra (*e.g.*, λ_{PL} = 645 nm and 716 nm for **CNPh-DMAC-TRZ** and **OMePh-DMAC-TRZ**, respectively).

The optical gap, $E_{0,0}(S_1)$ was determined from the intersection point of the tangents from the onsets of the absorption and emission spectra (Table **1**, Figure **S3-S8**). Generally, the $E_{0,0}$ energy increases from EDG to EWG, for example, $E_{0,0}$ = 2.29 and 2.70 eV for **OMePh-DMAC-TRZ** and **CNPh-DMAC-TRZ**, respectively, as demonstrated in Figure **4**.

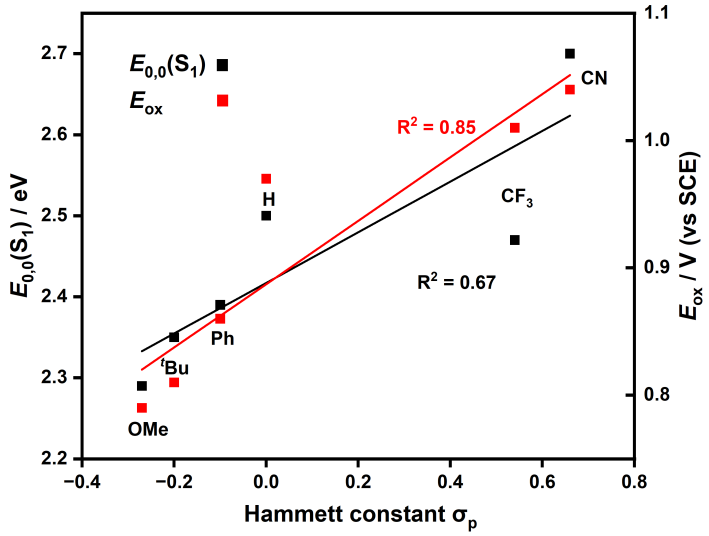

Figure **4**. Correlation of optical gap $E_{0,0}(S_1)$ and E_{ox} of the **DMAC-TRZ** derivatives with Hammett constant. The black R^2 corresponds to the black trendline associated with $E_{0,0}(S_1)$ and the red R^2 to the red trendline associated with E_{ox}.

Cyclic voltammetry (CV) and differential pulse voltammetry (DPV) revealed that **DMAC-TRZ** and its derivatives have similar reduction potentials, E_{red}, at *ca.* -1.58 V vs SCE in DMF (Figure **S9**), reflecting that reduction occurs on the triazine acceptor moiety and the donor groups are effectively electronically decoupled in the ground state. The E_{red} value in DMF is shifted anodically by *ca.* 100 mV relative to the E_{red} value previously reported in dichloromethane (E_{red} = -1.69 V vs SCE in DCM).[33] The limited electrochemical solvent window of DMF in the oxidation region prevented direct observation of the oxidation potential, E_{ox}. Rather, the E_{ox} values in DCM were used as a surrogate (Figure **S4**, Table **1**).[33] When changing from EDG to EWG substituted **DMAC-TRZ**, E_{ox} shifted anodically (*e.g.*, **OMePh-DMAC-TRZ**, E_{ox} = 0.79 V and **CNPh-DMAC-TRZ**, E_{ox} = 1.04 V), as shown in Figure **4**. From the electrochemical data, it can be concluded that all six **DMAC-TRZ**-based compounds are equally reducing in the $PC^{\bullet-}$ state, but $PC^{\bullet+}$ will become progressively more oxidizing as the substituent changes from EDG to EWG on the DMAC.

Despite having effectively the same E_{red} values, the six compounds display a range of E^*_{red} values (Table **1**) due to the varying $E_{0,0}$. The **DMAC-TRZ** derivatives become more potent photooxidants when changing from EDG (**OMePh-DMAC-TRZ**, E^*_{red} = 0.71 V) to EWG (**CNPh-DMAC-TRZ**, E^*_{red} = 1.12 V); however, show similar E^*_{ox} values (-1.46 V to -1.54 V) due to compensatory changes in E_{ox} and $E_{0,0}$. The outlier compound, **CNPh-DMAC-**

TRZ, is significantly more photoreducing (E^*_{ox} = -1.66 V), comparable to *fac*-Ir(ppy)$_3$ (E^*_{ox} = -1.70 V), although is less photoreducing than **PTH** (E^*_{ox} = -2.10 V).[8]

The time-resolved photoluminescence decays were obtained for a subset of the **DMAC-TRZ** derivatives in DMF under N_2 and air (Figures **S11-14**). As is characteristic of TADF compounds, the emission decays with biexponential kinetics associated with direct radiative decay from the S_1 state and delayed emission originating from the same state following intersystem crossing/reverse intersystem crossing cycles. Under deaerated conditions, the prompt lifetimes, τ_p, of **DMAC-TRZ**, **CF$_3$Ph-DMAC-TRZ** and **CNPh-DMAC-TRZ**, are in the nanosecond region (3.2 – 5.2 ns, Table **1**), while the delayed lifetimes, τ_d, are in the microsecond regime (0.2 – 0.9 μs). These compounds retain the delayed emission even under air, although τ_d decreases dramatically to 52 – 65 ns.

Table **1**. Optoelectronic properties of **DMAC-TRZ** and its derivatives.[a]

Compound	λ_{PL} / nm	$E_{0,0}$ / eV	E_{ox} / V [b]	E_{red} / V	E^*_{ox} / V [c]	E^*_{red} / V	τ_p / ns	τ_d / ns
DMAC-TRZ	655	2.50	0.97	-1.59	-1.53	0.91	3.2 (2.3)	954 (52)
OMePh-DMAC-TRZ	716	2.29	0.79	-1.58	-1.50	0.71		
^{t}BuPh-DMAC-TRZ	682	2.35	0.81	-1.58	-1.54	0.77		
dPh-DMAC-TRZ	683	2.39	0.86	-1.58	-1.53	0.81		
CF_3Ph-DMAC-TRZ	644	2.47	1.01	-1.57	-1.46	0.90	4.1 (3.8)	260 (65)
CNPh-DMAC-TRZ	645	2.70	1.04	-1.58	-1.66	1.12	5.2 (4.8)	810 (62)

[a] Values are reported in DMF unless otherwise noted. $E_{0,0}$ determined from the intersection point from the tangents of the onsets of the absorption and emission spectra. Redox potentials are reported vs SCE and are obtained from the maxima of the oxidation and reduction waves from the DPV. $E_{ox}^* = E_{ox} - E_{0,0}$ and $E_{red}^* = E_{red} + E_{0,0}$. τ_p and τ_d refer to prompt and delayed lifetimes, respectively. Lifetimes are obtained under N_2, with the value in parentheses being obtained under air. [b] Obtained in DCM. [c] Calculated using the E_{ox} value in DCM and the $E_{0,0}$ value in DMF.

Photochemical dehalogenation of aryl halides

The photoreducing ability of these compounds was probed in the dehalogenation of aryl halides, initially using methyl 4-chlorobenzoate (E_{red} = -1.98 V in DMF vs SCE) as a model substrate. Reaction yields were determined by GC-MS; the PCs were not detectable using this method. Replicating closely the conditions of Discekici *et al*., namely MeCN as solvent, NBu_3 and HCO_2H as additives, and 5 mol% of PC, the literature yield using **PTH** (94%) was higher than that achieved by us (77% Table **2**, entry 1), likely owing to the different reaction times (72 h vs 18 h, respectively). However, since most literature reports use only an amine as the additive (Figure **1b**), which is often DIPEA, the reaction conditions were modified to omit the acid and replace NBu_3 with DIPEA, resulting in a 42% yield with **PTH** (Table **2**, entry 2). As the **DMAC-TRZ** derivatives are not soluble in MeCN, the solvent was changed to DMF, giving a 78% yield (Table **2**, entry 3). Finally, at a reduced PC loading of 1 mol% of **PTH**, the yield decreased to 61% (Table **2**, entry 4).

The **DMAC-TRZ** derivatives were then trialled in the reaction using these conditions (DIPEA as the additive, DMF the solvent and 1 mol% of PC). Pleasingly, all compounds dehalogenated the substrate (Table **1**, entries 5-10), and the substituted **DMAC-TRZ** derivatives afforded higher product yields than **DMAC-TRZ** (55-100% and 43%, respectively). The GC-MS yields were highest with derivatives possessing EWGs, which may

be a consequence of these being more absorptive at the excitation wavelength (390 nm, Figure **3a**); this may influence the reaction kinetics. Thus, the dehalogenation of the substrate using **OMePh-DMAC-TRZ** as the PC was conducted for 48 h, resulting in an improvement in yield from 55% (18 h irradiation) to 70% (Table **2**, entry 11). Control reactions indicated that no product is formed in the absence of PC, amine, or light (Table **2**, entries 12-14).

Table **2**. GC-MS yields obtained for the **DMAC-TRZ** derivatives in the dehalogenation of methyl 4-chlorobenzoate.[a]

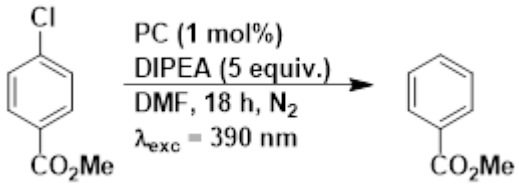

Entry	PC	GC-MS yield/ %
1	**PTH**	77 ± 1 [b]
2	**PTH**	42 ± 4 [c]
3	**PTH**	78 ± 4 [d]
4	**PTH**	61 ± 4 (17 ± 1)
5	**DMAC-TRZ**	43 ± 2 (36 ± 0)
6	**OMePh-DMAC-TRZ**	55 ± 3 (2 ± 2)
7	**^{t}BuPh-DMAC-TRZ**	64 ± 0 (79 ± 2)
8	**dPh-DMAC-TRZ**	100 ± 4 (100 ± 2)
9	**CF_3Ph-DMAC-TRZ**	98 ± 2 (94 ± 2)
10	**CNPh-DMAC-TRZ**	100 ± 0 (98 ± 2)
11	**OMePh-DMAC-TRZ**	70 ± 0 [e]
12	None	0 ± 0
13	**DMAC-TRZ**	0 ± 0 [f]
14	**DMAC-TRZ**	0 ± 0 [g]

[a] Reaction conditions: aryl halide (1 equiv., 0.1 mmol), PC (1 mol%) DIPEA (5 equiv.) and DMF (1 mL) at room temperature under N_2 for 18 h with irradiation from 390 nm Kessil LED. GC-MS yields were determined using mesitylene as an internal standard. Values in parentheses were conducted under aerated conditions. [b] 5 mol% of PC, NBu_3 (5 equiv.) and HCO_2H (5 equiv.) and MeCN were used under N_2. [c] 5 mol% of PC, DIPEA (5 equiv.) and MeCN were used under N_2. [d] 5 mol% of PC, DIPEA (5 equiv.) and DMF were used under N_2. [e] 48 h reaction time. [f] No light. [g] No amine.

To increase the dehalogenation yield with **DMAC-TRZ**, other amines, PC loadings and solvents were screened (Table **S2** and **S3**); however, no improvement in product yield was observed. Additionally, the tolerance of the reaction to air was investigated; all PCs, except **OMePh-DMAC-TRZ**, performed equally well under aerated conditions (Table **2**, entries 5-10). Therefore, subsequent reaction scope was conducted using DIPEA as the amine, DMF as the solvent, and aerated conditions.

All **DMAC-TRZ** derivatives were assessed in the substrate scope, except for **OMePh-DMAC-TRZ**, which was not tolerant to air under the reaction conditions, and the performance was cross compared with **4CzIPN** and **PTH**. The dehalogenation of aryl bromides and chlorides bearing EWGs, (E_{red} = -1.88 V – -2.04 V vs SCE, Figure **5a-d**), was first considered. Methyl 4-chlorobenzoate and 4-chlorobenzonitrile have previously been dehalogenated by PTH at 5 mol% loading, irradiated at 380 nm over 72 h, with NBu_3 and HCO_2H as the additives in MeCN, to give 94 and 94% yield, respectively.[8] As discussed above, replicating these conditions but with a shorter reaction time of 18 h, produced a 77% yield of methyl benzoate from methyl 4-chlorobenzoate. Instead, under the optimized conditions identified for the **DMAC-TRZ** derivatives, the use of **PTH** yielded only 17 and 13% of the dehalogenated product, respectively, from methyl 4-chlorobenzoate and 4-chlorobenzonitrile. The **DMAC-TRZ** derivatives yielded high quantities of the dehalogenated products under these conditions, particularly **CNPh-DMAC-TRZ**, which quantitatively dehalogenated these two substrates. In fact, the use of **CNPh-DMAC-TRZ** yielded 88 – 100% of the target product for all four substrates with E_{red} of -1.88 V to -2.04 V (Figure **5**). **CF_3Ph-DMAC-TRZ** and **dPh-DMAC-TRZ** also performed moderate to excellently for these substrates (50 – 94% and 45 – 100% yield, respectively), **^{t}BuPh-DMAC-TRZ** tended to give lower yields (35 – 79%) and **DMAC-TRZ** was the least efficient (8 – 36%). Importantly, across all substrates, at least one of the **DMAC-TRZ** derivatives afforded a greater yield than **4CzIPN** and **PTH**.

We next attempted the dehalogenation of more demanding aryl halides bearing conjugative or EDGs. The dehalogenation of 4-chlorobiphenyl (E_{red} = -2.43 V, Figure **5e**) was screened; **dPh-DMAC-TRZ**, **CF_3Ph-DMAC-TRZ** and **CNPh-DMAC-TRZ** afforded low yields of product (36, 32 and 20%, respectively). **^{t}BuPh-DMAC-TRZ** performed even worse (8%) while **DMAC-TRZ** did not produce any reaction. The use of **4CzIPN** or **PTH** resulted in <5% of product. The low yields obtained are tentatively attributed to alternative side reactions that seem to proceed with this substrate; for example, with **CNPh-DMAC-TRZ** the gas chromatogram shows two additional peaks beside the starting material and product in

comparison to the spot-to-spot conversion typically observed for the other substrates. The dehalogenation of 4-iodoanisole (E_{red} = -2.50 V, Figure **5f**) has been reported in the literature using **PTH** (with the conditions previously mentioned), giving 92% yield in 5 h under N_2, or 89% in 24 h under air.[8] Under our optimized conditions, **PTH** yields only 14% of the product, which is marginally better than the 7% yield achieved with **DMAC-TRZ**. By contrast, a progressively increasing yield from 27 to 61% was observed for the **DMAC-TRZ** derivatives, which was correlated to the Hammett constant (Figure **5f**). **4CzIPN** afforded similar yields to **CNPh-DMAC-TRZ** (58 and 61%, respectively).

The most challenging two substrates to dehalogenate that we investigated were 3-bromoanisole (E_{red} = -2.59 V) and 4-bromoanisole (E_{red} = -2.72 V). With respect to the first substrate, low yields of 2, 9, 10 and 23% were obtained when using **4CzIPN**, **dPh-DMAC-TRZ**, **CF_3Ph-DMAC-TRZ** and **CNPh-DMAC-TRZ**, respectively, while no product was formed with **DMAC-TRZ**, **^{t}BuPh-DMAC-TRZ** and **PTH** (Figure **5g**). Increasing the reaction time to 72 h resulted in a considerably increased product yield of 13, 40, 27 and 71% using **^{t}BuPh-DMAC-TRZ**, **dPh-DMAC-TRZ**, **CF_3Ph-DMAC-TRZ** and **CNPh-DMAC-TRZ**, respectively. By contrast, the product yield increased only incrementally with **4CzIPN** (10%) while no product formed with **DMAC-TRZ** or **PTH**. The dehalogenation of 4-bromoanisole has previously been reported using **[^{t}Bu-Mes-Acr]BF_4** in a yield of 90% using 10 mol% of PC, MeCN as the solvent and 16 h irradiation time under N_2.[9,34] Unsurprisingly, neither **DMAC-TRZ** nor **PTH** could dehalogenate 4-bromoanisole, but each of **^{t}BuPh-DMAC-TRZ**, **dPh-DMAC-TRZ**, **CF_3Ph-DMAC-TRZ** and **CNPh-DMAC-TRZ** produced anisole in 9, 26, 18 and 30% yield, respectively, over 72 h (Figure **6h**), yields which are all equivalent to or higher than that achieved with **4CzIPN** (10%). None of the PCs tested (the **DMAC-TRZ** derivatives, **4CzIPN** or **PTH)** could dehalogenate 4-chloroanisole (E_{red} = -2.90 V), even after 72 h, indicating a limit of the reduction capability of these PCs.

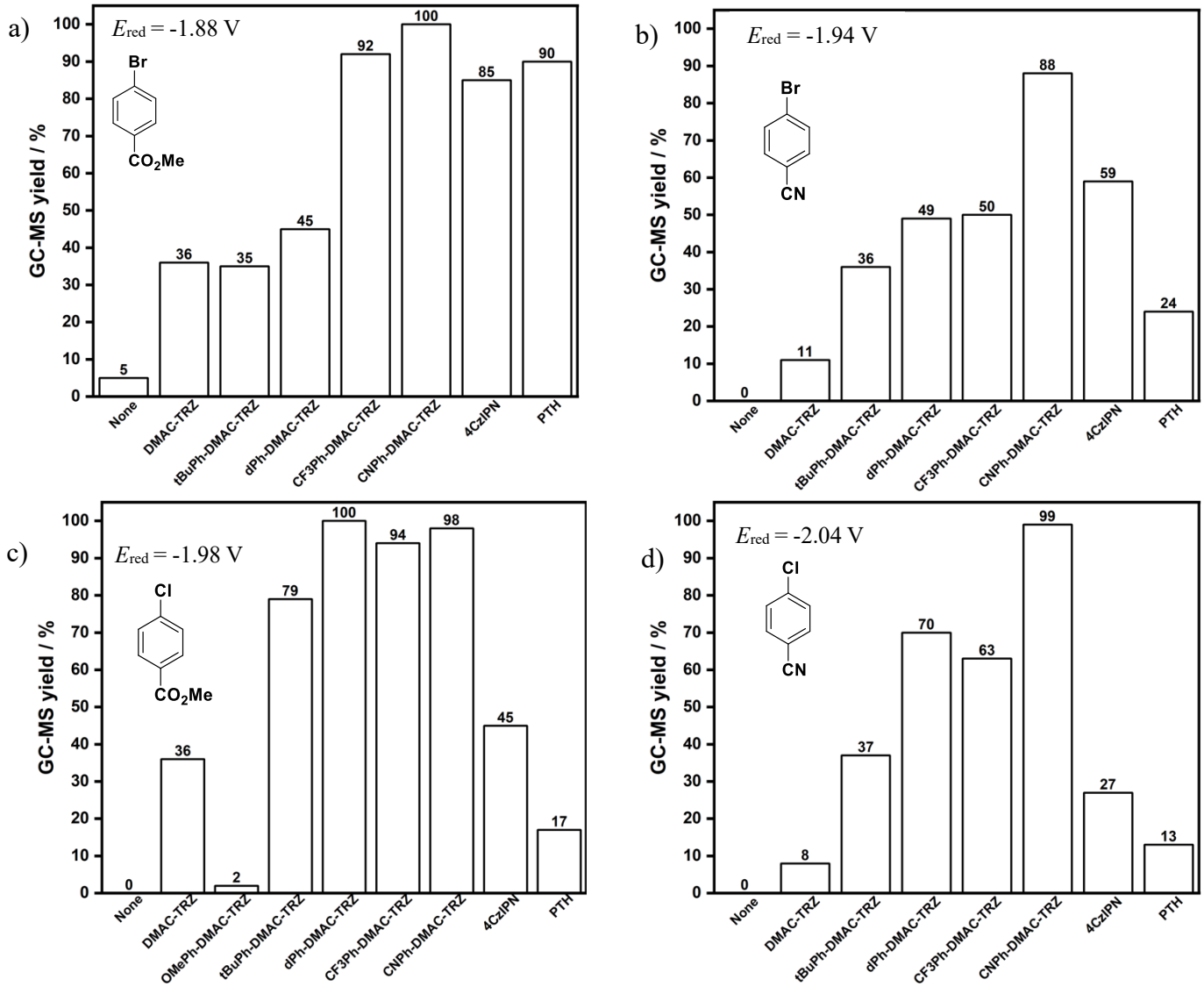

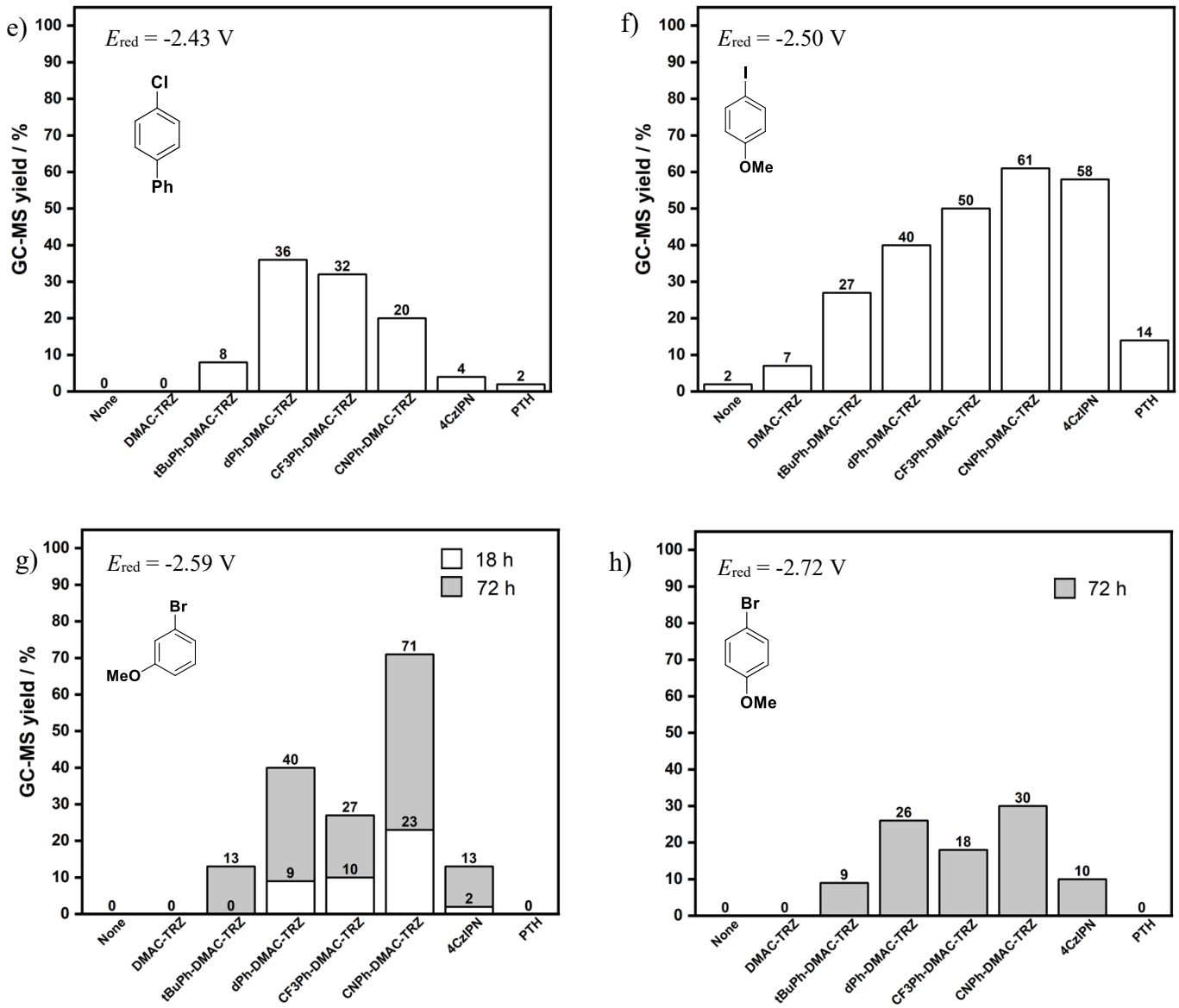

Figure **5**. GC-MS yields of dehalogenated products using either no PC or one of **DMAC-TRZ**, **^{t}BuPh-DMAC-TRZ**, **dPh-DMAC-TRZ**, **CF_3Ph-DMAC-TRZ**, **CNPh-DMAC-TRZ**, **4CzIPN** and **PTH**. Reaction conditions unless otherwise stated: aryl halide (1 equiv., 0.1 mmol), PC (1 mol%) DIPEA (5 equiv.) and DMF (1 mL) at room temperature under air for 18 h with irradiation from 390 nm Kessil LED. GC-MS yields were determined using mesitylene or 1,3,5-trimethoxybenzene as the internal standard. All redox potentials are quoted vs SCE and are from Ref [16,18–20,22]. a) Reaction was conducted under N_2. g) Reaction was conducted for 18 h and 72 h. h) Reaction conducted for 72 h.

Mechanistic investigation

Except for **CNPh-DMAC-TRZ** (E^*_{ox} = -1.66 V) the **DMAC-TRZ** derivatives tend to be equally strong photoreductants (E^*_{ox} = -1.46 V to -1.54 V) yet produced remarkably divergent yields across the substrates. Additionally, none of the PCs investigated should be thermodynamically capable of directly photoreducing the substrates. These two factors imply that these compounds cannot operate via an oxidative quenching mechanism, as proposed for **PTH**,[8] leading us to instead consider the conPET mechanism.[7,9,11] For subsequent mechanistic investigation, we focused on **CF_3Ph-DMAC-TRZ** and **CNPh-DMAC-TRZ**, since these tended to afford the greatest yields of dehalogenated product, as well as **DMAC-TRZ** as a reference comparison.

Stern-Volmer quenching studies were conducted using the model system of methyl 4-chlorobenzoate and DIPEA. To our surprise, no discernible quenching could be observed for **DMAC-TRZ**, **CF_3Ph-DMAC-TRZ** or **CNPh-DMAC-TRZ** (Figures **S16-18**). This raised the question of the photostability, thus UV-Vis absorption spectra were measured before and after irradiation of the PC in DMF, as well as in the presence of only DIPEA and under the dehalogenation conditions of methyl 4-chlorobenzoate. The pre-irradiation profiles in all cases are reflective of the UV-Vis absorption spectrum of the PC; therefore, spectroscopic changes observed after irradiation can be assigned to changes to the structure of the PC (Figure **S25-S29**).

Changes in the absorption spectra were observed for all **DMAC-TRZ** PCs, **4CzIPN** and **PTH** upon irradiation of the PC in DMF Figure 6). For the **DMAC-TRZ** derivatives, a loss of the both the low-energy CT and LE bands were observed, causing a dramatic blue-shift of the absorption profile. Similarly, **4CzIPN** showed a blue-shifted absorption spectrum, and an absence of the characteristic CT band between 350-450 nm. By contrast, **PTH** developed two new bands (302 and 338 nm) and the absorption onset was unaffected, suggesting that decomposition had only partially occurred for this PC. After irradiation in the presence of DIPEA in DMF, changes distinct from those seen when simply irradiating the PC were observed. For **DMAC-TRZ** and **PTH**, this was manifested in the growth of a new band at *ca.* 415 nm. For **CF_3Ph-DMAC-TRZ**, the absorption spectrum was like that pre-irradiation, but with a blue-shift in the LE band (357 nm) and the absorption onset. Pleasingly, **CNPh-DMAC-TRZ** appeared to be relatively photostable with minimal changes observed in the absorption spectrum. **4CzIPN** displayed the same significant blue-shift in its absorption profile as was

observed when only irradiated in DMF. Finally, the UV-Vis absorption spectra were obtained before and after irradiation under the reaction conditions of the dehalogenation of methyl 4-chlorobenzoate. **4CzIPN** again displayed the same post-irradiation profile, suggesting the same photodegradation product is formed irrespective of the presence of DIPEA and methyl 4-chlorobenzoate. **PTH** also displayed a similar post irradiation profile to that observed after irradiation in the presence of DIPEA, implying that DIPEA plays a role in the photodegradation of **PTH** that forms degradation product(s) distinct from those obtained from only irradiating **PTH**. For **CF_3Ph-DMAC-TRZ** and **CNPh-DMAC-TRZ**, and to a lesser extent, **DMAC-TRZ**, a red-shift in the absorption onset is observed; for **CF_3Ph-DMAC-TRZ** and **CNPh-DMAC-TRZ**, the well-resolved LE band at 357 and 378 nm, respectively, becomes broad and less well defined.

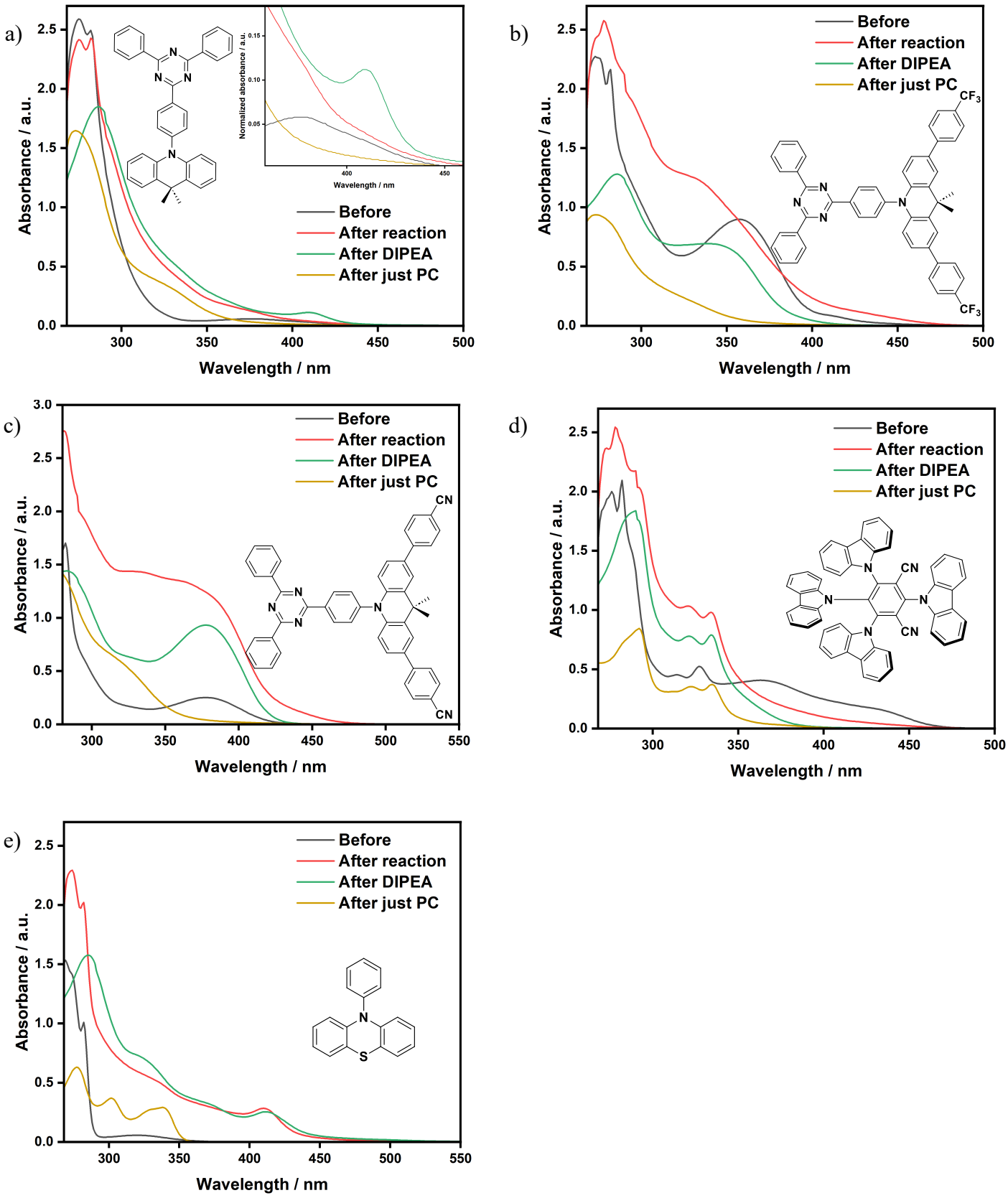

Figure **6**. UV-Vis absorption spectra before and after irradiation in the dehalogenation of methyl 4-chlorobenzoate, and after irradiation in the presence of DIPEA and after irradiation

of just the PC, all in DMF using a 390 nm Kessil lamp for 18 h. a) **DMAC-TRZ**, b) **CF_3Ph-DMAC-TRZ**, c) **CNPh-DMAC-TRZ**, d) **4CzIPN** and e) **PTH**.

Recognising the non-innocence of DMF in the dehalogenation process, we consulted the previous photocatalysis literature employing this solvent. Using TiO_2 as the PC, DMF can be photocatalytically decomposed to carbon monoxide and dimethylamine under UV light irradiation (λ_{exc} = 365 nm).[35] In the presence of water vapour, using a metal-organic-framework PC and visible light irradiation (26 W helical light bulb), the decomposition products of DMF were instead proposed to be formic acid and dimethylamine.[36,37] It is clear that under certain conditions, DMF is not a benign solvent for photocatalysis reactions. We thus attempted to understand its influence on the photodegradation of model PCs **4CzIPN** and **DMAC-TRZ**.

To isolate the photodegradation products, **4CzIPN** was irradiated in DMF for 18 h at five times the reaction scale, which led to complete depletion of **4CzIPN** (Figure **S37** and **S42**). Following purification attempts, carbazole was isolated, as confirmed by ^{1}H NMR and GC-MS (Figures **S38**, **S40** and **S41**); further, the UV-Vis absorption spectrum of carbazole in DMF mirrors quite closely the post-irradiation UV-Vis absorption spectrum of **4CzIPN** (Figure **S31**). The GC-MS shows an additional peak with *m/z* of 195 (Figure **S40** and **S41**). Based on this mass and on the ^{1}H NMR spectrum (Figure **S39**), we tentatively assigned the identity of this species as *N*-formylcarbazole based on a cross-comparison with the spectrum from the literature.[38] Other products could neither be cleanly isolated nor identified.

A similar experiment was conducted with **DMAC-TRZ** (*i.e.* irradiation at five times the reaction scale); however, no photodegradation was observed by UV-Vis absorption spectroscopy. To interrogate this discrepancy in behaviour, steady-state PL spectra were obtained for the post-irradiation profile of **DMAC-TRZ** irradiated in DMF at the scale used in the dehalogenation reaction and at five times the scale (Figure **7**). After irradiation at normal scale, the emission is considerably blue-shifted (λ_{PL} = 486 nm compared to 655 nm for **DMAC-TRZ** in DMF), while the post-irradiation profile conducted at five times the normal scale shows an emission spectrum that is largely reflective of **DMAC-TRZ**; a small shoulder is observed between 400 – 500 nm. After irradiation of methyl 4-chlorobenzoate in the presence of DIPEA, using **DMAC-TRZ** as the PC, both at the normal reaction scale and five times the normal reaction scale, the emission profiles are almost identical, with λ_{PL} of 455 nm (Figure **7**). This indicates that irrespective of the scale used, **DMAC-TRZ** photodegrades consistently in the

dehalogenation reaction, and that this degradation is distinct to that observed when **DMAC-TRZ** is photoexcited in DMF. These degradation products are not DMAC or triazine, based on a cross-comparison of their respective emission spectra (Figure **7**).

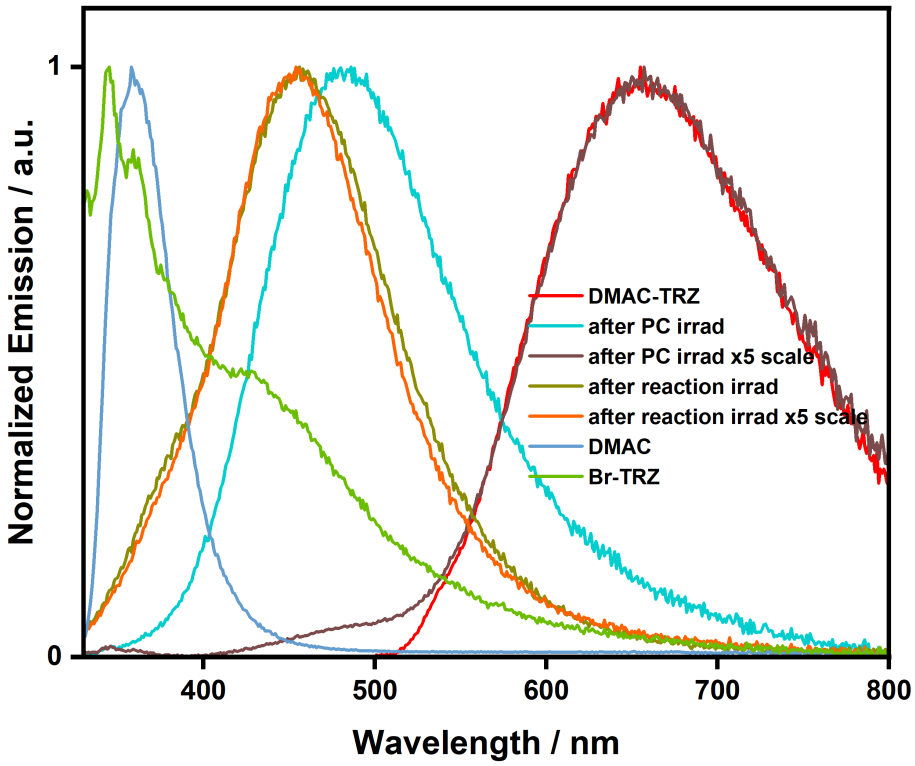

Figure **7**. Normalized steady-state PL of **DMAC-TRZ** in DMF and of **DMAC-TRZ** after irradiation in DMF (at normal reaction scale and 5× the normal scale) as well as the post-irradiation profile of the reaction mixture (methyl 4-chlorobenzoate, DIPEA, **DMAC-TRZ** in DMF) at normal scale and at 5× the normal scale. All irradiation conducted with a 390 nm Kessil LED excitation source. For PL spectra, λ_{exc} = 290 nm.

These studies lead us to conclude that the family of **DMAC-TRZ** derivatives photodegrades into species that are sufficiently photoreducing to promote the dehalogenation of the aryl halides; we were unable to either isolate or characterize these photodegradation products. The poor photostability observed for all PCs investigated, including literature PCs, raises the question of whether these compounds can be classified as PCs, or whether they are better described as pre(photo)catalysts.

Conclusions

A series of five donor-acceptor TADF compounds were developed to target the photoreduction of aryl halides. Modification of the donor group of the parent compound **DMAC-TRZ** with a Hammett series of *p*-substituted phenyl moieties, resulted in significant changes to the optoelectronic properties. For example, E_{ox} varied from 0.97 V for the parent compound, to 0.79-1.04 V, depending on whether the donor was substituted with an aryl substituent bearing an EDG or EWG. Consequently, E^*_{ox} ranged from -1.46 V to -1.66 V, with the most photoreducing derivative, **CNPh-DMAC-TRZ** (E^*_{ox} = -1.66 V), comparable to *fac*-Ir(ppy)$_3$ (E^*_{ox} = -1.70 V).

All five of the substituted **DMAC-TRZ** derivatives proved to be more potent PCs than the parent compound and could dehalogenate aryl halides with E_{red} ranging from -1.88 to -2.72 V vs SCE. Particularly, **CF$_3$Ph-DMAC-TRZ** and **CNPh-DMAC-TRZ** provided the highest yields, with the latter achieving yields of 30-71% for substrates with E_{red} < -2.5 V. Although these yields are lower than those reported for similar substrates using **[^{t}Bu-Mes-Acr]BF$_4$**,[9] our photocatalysis conditions proceed under air and at lower PC loading (1 mol%). Mechanistically however, all PCs photodegrade under the reaction conditions, with the resultant photodegradation product responsible for the required dehalogenation.

Acknowledgements

We are grateful to the University of St Andrews, Syngenta, and the EPSRC Centre for Doctoral Training in Critical Resource Catalysis (CRITICAT) for financial support [Ph.D. studentship to "M.A.B."; Grant code: EP/L016419/1]. E.Z.-C. acknowledges EPSRC for support (EP/W007517/1). This project has received funding from the European Union's Horizon 2020 research and innovation programme under the Marie Skłodowska Curie grant agreement No 812872 (TADFlife). We are thankful to the SFC Saltire Emerging Researcher Scheme for funding the placement of M.A.B to the A.S. lab. We thank Umicore AG for the gift of materials.

Supporting Information

Electronic supplementary information available: electrochemistry, time resolved emission spectra, Stern-Volmer quenching studies, photostability studies, photocatalysis procedures, yields for all reactions and GC-MS calibration curves.

References

[1] G. E. M. Crisenza, P. Melchiorre, *Nat. Commun.* **2020**, *11*, 803–806.

[2] R. C. McAtee, E. J. McClain, C. R. J. Stephenson, *Trends Chem.* **2019**, *1*, 111–125.

[3] N. A. Romero, D. A. Nicewicz, *Chem. Rev.* **2016**, 10075–10166.

[4] N. Kvasovs, V. Gevorgyan, *Chem. Soc. Rev.* **2021**, *50*, 2244–2259.

[5] H. G. Kuivila, *Acc. Chem. Res.* **1968**, *1*, 299–305.

[6] A. M. Rosa, A. M. Lobe, P. S. Branco, S. Prabhakar, *Tetrahedron* **1997**, *53*, 285–298.

[7] I. Ghosh, T. Ghosh, J. Bardagi, B. Konig, *Science* **2014**, *346*, 725–728.

[8] E. H. Discekici, N. J. Treat, S. O. Poelma, K. M. Mattson, Z. M. Hudson, Y. Luo, C. J. Hawker, J. R. De Alaniz, *Chem. Commun.* **2015**, *51*, 11705–11708.

[9] I. A. MacKenzie, L. Wang, N. P. R. Onuska, O. F. Williams, K. Begam, A. M. Moran, B. D. Dunietz, D. A. Nicewicz, *Nature* **2020**, *580*, 76–80.

[10] Y. Kwon, J. Lee, Y. Noh, D. Kim, Y. Lee, C. Yu, J. C. Roldao, S. Feng, J. Gierschner, R. Wannemacher, M. S. Kwon, *Nat. Commun.* **2023**, *14*, 92.

[11] J. Xu, J. Cao, X. Wu, H. Wang, X. Yang, X. Tang, R. W. Toh, R. Zhou, E. K. L. Yeow, J. Wu, *J. Am. Chem. Soc.* **2021**, *143*, 13266–13273.

[12] T. Pavlovska, D. Král Lesný, E. Svobodová, I. Hoskovcová, N. Archipowa, R. J. Kutta, R. Cibulka, *Chem. Eur. J.* **2022**, *28*, e202200768.

[13] T. Bortolato, G. Simionato, M. Vayer, C. Rosso, L. Paoloni, E. M. Benetti, A. Sartorel, D. Lebœuf, L. Dell'Amico, *J. Am. Chem. Soc.* **2023**, *145*, 1835–1846.

[14] B. Pfund, V. Hutskalova, C. Sparr, O. S. Wenger, *Chem. Sci.* **2023**, 11180–11191.

[15] S. Halder, S. Mandal, A. Kundu, B. Mandal, D. Adhikari, *J. Am. Chem. Soc.* **2023**, *145*, 22403–22412.

[16] I. Reche, S. Mena, I. Gallardo, G. Guirado, *Electrochim. Acta* **2019**, *320*, 134576.

[17] C. Combellas, F. Kanoufi, J. Pinson, F. I. Podvorica, *Electrochem. Commun.* **2019**, *98*, 119–123.

[18] T. U. Connell, C. L. Fraser, M. L. Czyz, Z. M. Smith, D. J. Hayne, E. H. Doeven, J. Agugiaro, D. J. D. Wilson, J. L. Adcock, A. D. Scully, D. E. Gomez, N. W. Barnett, A. Polyzos, P. S. Francis, *J. Am. Chem. Soc.* **2019**, *141*, 17646–17658.

[19] C. Costentin, M. Robert, J. Save, *J. Am. Chem. Soc.* **2004**, *126*, 16051–16057.

[20] G. B. Gavioli, M. Borsari, C. Fontanesi, *J. Chem. Soc. Faraday Trans.* **1993**, *89*, 3931–3939.

[21] A further discussion of organic PCs used in the last year for the photoinduced dehalogenation of aryl halides is presented in the Supporting Information.

[22] F. Glaser, O. S. Wenger, *J. Am. Chem. Soc. Au* **2022**, *2*, 1488–1503.

[23] H. Kim, H. Kim, T. H. Lambert, S. Lin, *J. Am. Chem. Soc.* **2020**, *142*, 2087–2092.

[24] M. A. Bryden, E. Zysman-Colman, *Chem. Soc. Rev.* **2021**, *50*, 7587–7680.

[25] M. A. Bryden, F. Millward, T. Matulaitis, D. Chen, M. Villa, A. Fermi, S. Cetin, P. Ceroni, E. Zysman-Colman, *J. Org. Chem.* **2023**, *88*, 6364–6373.

[26] C. Prentice, J. Morrison, A. D. Smith, E. Zysman-Colman, *Chem. Eur. J.* **2022**, *29*, e202202998.

[27] E. Sauve, D. Mayder, S. Kamal, M. S. Oderinde, Z. Hudson, *Chem. Sci.* **2022**, *13*, 2296–2302.

[28] SciFinder search for ‘4CzIPN’ and ‘catalyst use,’” can be found under https://scifinder-n.cas.org/search/reference/64d6090282afe1695aecadb2/1. Date accessed: 11/08/2023.

[29] M. Y. Wong, E. Zysman-Colman, *Adv. Mater.* **2017**, *29*, 1605444.

[30] W. L. Tsai, M. H. Huang, W. K. Lee, Y. J. Hsu, K. C. Pan, Y. H. Huang, H. C. Ting, M. Sarma, Y. Y. Ho, H. C. Hu, C. C. Chen, M. T. Lee, K. T. Wong, C. C. Wu, *Chem. Commun.* **2015**, *51*, 13662–13665.

[31] Sigma Aldrich website. Date accessed: 10/08/2023.

[32] We note that structurally similar 9,10-dihydro-9,9-dimethylacridine/2,4,6-triphenylpyrimidine have been used as photosensitizers in a photopolymerization reaction in Polymer Chem., 2022, 13, 3892- 3903.

[33] E. Crovini, K. Stravou, P. Sahay, B. M. Nguyen, T. Comerford, S. Warriner, W. Brutting, A. Monkman, E. Zysman-Colman, *ChemRxiv.* **2024**, DOI 10.26434/chemrxiv-2024-htwbt.

[34] All attempts to recreate this yield in our set-up, according to the reported conditions,

unfortunately failed.

[35] X. Feng, Z. Li, *J. Photochem. Photobiol. A Chem.* **2017**, *337*, 19–24.

[36] P. Xue, J. Huang, L. Lin, R. Li, M. Tang, Z. Wang, *Mol. Catal.* **2021**, *506*, 111542.

[37] However, this reaction was also heated to 90 °C and it is unclear if the degradation of DMF stems from the light or the heat.

[38] Z. Qiu, S. Nakamura, K. Fujimoto, *Org. Biomol. Chem.* **2019**, *17*, 6277–6283.

TOC: